

Presence of parimagnetism in HoCo₂ under hydrostatic pressure

J Valenta¹, J Prchal¹, R Khasanov², M Kratochvílová¹, M Míšek¹, M Vališka¹ and V Sechovský¹

¹ Charles University in Prague, Faculty of Mathematics and Physics, DCMP, Ke Karlovu 5, 121 116 Praha 2, Czech Republic

² Laboratory for muon Spin Spectroscopy, Paul Scherrer Institute, CH-5232, Villigen PSI, Switzerland

E-mail: valeja@mag.mff.cuni.cz

Abstract. This paper deals with a pressure evolution of newly observed phenomenon – parimagnetism in HoCo₂. HoCo₂ containing localized Ho magnetic moments and itinerant Co magnetic moments order ferrimagnetically below $T_C = 79.5$ K at ambient pressure. The corresponding Ho and Co magnetic sublattices are ferromagnetic and coupled mutually antiparallel. In paramagnetic range, the Co moments form ferromagnetic clusters which hold short range antiparallel configuration with the nearest Ho moments at temperatures up to the flipping temperature $T_f = 125$ K. The decay of Co clusters was observed by muon spin relaxation spectroscopy (μ SR) at $T^* \sim 170$ K. Our results of AC-magnetic susceptibility and zero-field μ SR measurements of HoCo₂ at ambient and hydrostatic pressures presented in this paper reveal strong pressure dependence of the characteristic temperatures which is closely related to the itinerant character of Co magnetism and variations of exchange interactions.

1. Introduction

HoCo₂ belongs to the group of intermetallic RCo₂ compounds forming a cubic Laves phase (MgCu₂-type, space group Fd-3m). The localized 4f electron magnetic moments of Ho ions coexist with the Co itinerant 3d electrons, which appear on the verge of magnetism. Application of external magnetic field on the Co sublattice approaching the megagauss range can induce a discontinuous splitting of the majority and minority 3d sub-bands, formation of Co magnetic moments and simultaneous freezing of 3d spin fluctuations as manifested for isostructural YCo₂ [1]. An analogous Co metamagnetic state may be achieved by employing a large exchange field due to the ferromagnetically ordered 4f magnetic moments in DyCo₂, HoCo₂ and ErCo₂ at T_C [2]. At temperatures below T_C the rare-earth and Co magnetic moments form a ferromagnetic sub-lattice, respectively. The two sub-lattices are coupled antiparallel.

Recently, nonzero Co magnetic moments have been revealed persisting at temperatures much higher than T_C in ErCo₂, HoCo₂, DyCo₂ and TmCo₂. With decreasing temperature the Co magnetic moments form small ferromagnetic clusters of the size comparable with a crystal unit cell. At temperatures below a so called flipping temperature $T_f > T_C$ ($T_{f, HoCo_2} \sim 125$ K) the net magnetization of Co magnetic clusters couples antiparallel to the Er, Ho, Dy or Tm magnetic moments, respectively. Formation of these short range *parimagnetic* configurations is reflected in an anomaly in temperature dependence of AC magnetic susceptibility at T_f [3-6]. Parimagnetism differs fundamentally from



conventional paramagnetism which is characterized by mutually independent behavior of individual permanent moments of magnetic ions yielding their entirely random orientations.

HoCo₂ undergoes an order-order magnetic phase transition T_R at which the magnetocrystalline anisotropy changes – the easy direction of magnetization changes from the [100] to [110] while cooling, which reflects temperature variation of the energy level scheme of the ⁵I₈ ground-state multiplet of the Ho³⁺ ion in the laves phase crystal field [7]. This transition is reflected in another anomaly in the temperature dependence of AC susceptibility.

External hydrostatic pressure usually reduces interatomic distances which have various impacts on magnetic moments and exchange interactions. This effect leads to reduction of Curie temperature for DyCo₂, HoCo₂, ErCo₂ and TmCo₂ [8-10]. For ErCo₂ a negative pressure effect on flipping temperature T_f has been observed with the rate of $dT_f/dp \sim -4.5$ K/GPa [10].

2. Experimental

The polycrystalline sample of HoCo₂ was produced by melting of stoichiometric mixture of Ho (3N) and Co (4N5) in a mono-arc furnace under argon protective atmosphere (6N). The sample was warped in a Ta foil and sealed under vacuum into a silica tube and annealed at 950 °C for 10 days. X-ray powder diffraction analysis shows small amount of HoCo₃ as impurity phase.

The AC-magnetic susceptibility was measured using a commercial Quantum Design MPMS magnetometer with pressure cell [11] up to 1 GPa. A spindle oil OL-3 was used as a liquid pressure transmitting medium and a small piece of lead was used as a pressure sensor. For pressures above 1 GPa up to 3 GPa, the double-layered (CuBe/NiCrAl) piston-cylinder pressure cell mounted in the closed-cycle refrigerator apparatus was used. We used Daphne oil 7373 as a liquid pressure-transmitting medium and a pressure dependent resistance of a manganin wire as a pressure sensor in this cell. AC-magnetic susceptibility was measured (in the latter mentioned cell) by using homemade miniature detection coil set that fits inside the sample space [10].

Experiments of μ SR were performed at the muon beam line at the Swiss muon source (μ S) at the Paul Scherrer Institute (PSI, Villigen) using General Purpose Decay-Channel Spectrometer (GPD). Hydrostatic pressure was generated by a single-layered piston-cylinder pressure cell (made of the NP35N alloy; with nominal pressure up to 2 GPa) mounted into He-flow cryostat. Daphne 7373 was used as a pressure transmitting medium and a pressure dependent temperature of the superconducting transition of indium was used for determination of pressure inside the cell.

In a μ SR experiment a muon beam (nearly 100% polarized) is implanted into the sample. After the muons thermalize with the sample, they occupy a specific position - usually an interstitial one – within the crystal lattice of the sample. The spin of muon interacts with the local magnetic field at the muon position. Muon decays after its lifetime (~ 2.2 μ s) into a positron, electron neutrino and muon antineutrino. The positron is emitted preferably into the direction of the muon spin direction. The emitted positrons are detected in time by the detectors which have position front (F) and back (B) towards the direction of muon beam. Histograms of each detector have a large number of counts and it is lead to determine “raw asymmetry” as function of time:

$$A(t) = \frac{N_F(t) - N_B(t)}{N_F(t) + N_B(t)}, \quad (1)$$

where $N_F(t)$ and $N_B(t)$ are the positron count rates for each detector.

3. Results

3.1. AC-magnetic susceptibility measurement

The temperature dependence of the AC susceptibility of HoCo₂ under hydrostatic pressure indicates presence of three magnetic phenomena. The main aspect is the first-order magnetic phase transition to

ferrimagnetic ordering at $T_C = 79.5$ K. At lower temperatures, there is observed a change of easy direction of magnetization at $T_R = 16.4$ K. Finally, the onset of paramagnetism produces an AC-susceptibility anomaly around $T_f \sim 125$ K. Figure 1 shows the measured curve of AC-magnetic susceptibility at around 0.5 GPa. Temperature T_R is determined as the top of first bump which is in good agreement with previous reports. Curie temperature is determined as the top of peak which is marked in figure 1 (temperature of this point is in good agreement with T_C determined from electric resistivity measurement in reference [8] for all measured pressures), and flipping temperature as the top of bump obtained by subtracting of the Curie-Weiss fit from the measured data in the paramagnetic region.

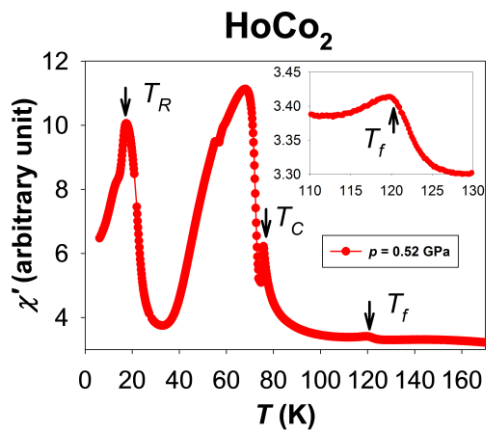


Figure 1. AC-magnetic susceptibility curve measured under hydrostatic pressure $p = 0.52$ GPa. The insert shows anomaly about 120 K in detail.

Increasing the hydrostatic pressure leads to a shift of all characteristic temperatures. The flipping temperature T_f and Curie temperature T_C shift towards lower temperatures ($dT_f/dp \sim -10$ K/GPa, $dT_C/dp \sim -13$ K/GPa), spin reorientation temperature shifts to higher temperature ($dT_R/dp \sim +4$ K/GPa) up to 3 GPa. The phase diagram constructed from the measured points is shown in figure 2.

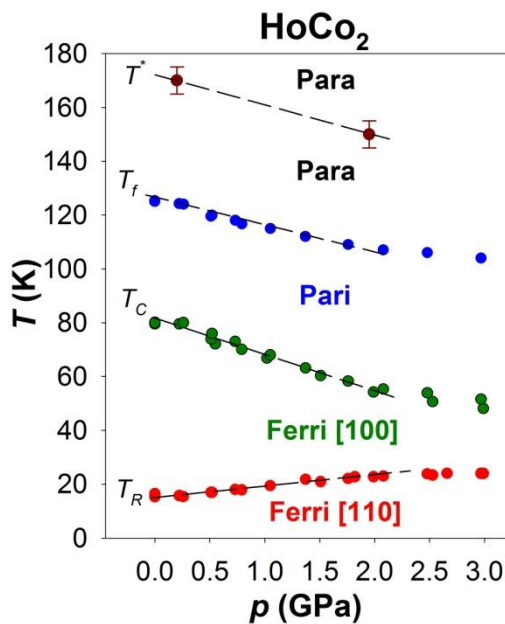


Figure 2. Pressure dependence of characteristic temperatures. Points of T_R , T_C and T_f are determined from AC-magnetic susceptibility measurements and points of T^* are determined from μ SR experiment.

3.2. μ SR experiment

In the paramagnetic regime, the μ SR spectrum can be fitted only with one exponential function for the polycrystalline sample:

$$A(t) = A_0 \exp(-\lambda_{par}t), \quad (2)$$

where A_0 is the initial asymmetry, t is time and $\lambda_{par} = \gamma_\mu^2 \langle B_\mu^2 \rangle \tau_C$ is the paramagnetic relaxation rate [12].

The measured data could not be fitted by the equation (2) between the Currie temperature T_C and a temperature T^* . The sum of two exponentials is more suitable expression for the fitting in this temperature range:

$$A(t) = A_{fast} \exp(-\lambda_{fast}t) + A_{slow} \exp(-\lambda_{slow}t), \quad (3)$$

where the first exponential on the right side corresponds to short-range-order correlation in paramagnetic region caused by Co magnetic clusters [12]. This component leads to a fast damping of μ SR spectrum with increasing time. The second exponential on the right side is dominant at longer times and corresponds to paramagnetic fluctuations of Ho magnetic moments. The results of fits are shown in figures 3 and 4 for different pressures.

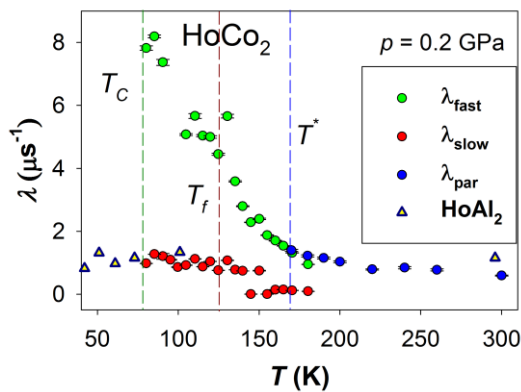


Figure 3. Results of fitted spectra measured from T_C to room temperature at pressure 0.2 GPa. The triangles representing data of HoAl_2 correspond to data taken from reference [13].

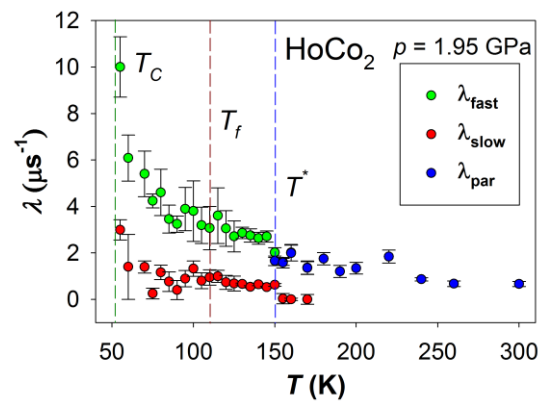


Figure 4. Results from fitted data measured from T_C to room temperature at pressure 1.95 GPa.

The figures 3 and 4 demonstrate that at a certain temperature, the λ_{fast} falls close to λ_{slow} and further on the use of the equation (2) is more suitable for fitting. This temperature marked as T^* corresponds to $T_{0.2}^* \sim 170$ K and $T_{1.95}^* \sim 150$ K for pressures $p = 0.2$ GPa and 1.95 GPa, respectively. Pressure development of T^* is included in the phase diagram (figure 2) and its pressure coefficient was estimated as $dT^*/dp \sim -11$ K/GPa.

4. Discussion

Experimental results show increase of T_R with pressure up to 3 GPa, as can be seen in figure 2. The parameters of the crystal field acting on the Ho^{3+} ion in HoCo_2 is which decides about the easy magnetization direction is temperature dependent because of thermal expansion, which is invar-like at temperatures below T_C owing to spontaneous magnetostriction [14]. When reducing lattice volume by applying hydrostatic pressure one would expect decrease of T_C . Contrary a T_R increase has been observed. Consistent explanation of the virtually surprising result requires relevant ab initio electronic

structure calculations including the effect of pressure induced changes of the Co 3d charge density on crystal field parameters.

Increasing pressure causes broadening of the Co 3d band and consequently the Co magnetic moment becomes diminished that leads to rapid decreasing T_C . For pressures higher than the critical pressure $p_C > 4$ GPa the ordered Co moment vanishes because the Ho-Co exchange interaction already cannot split the Co 3d up and down sub-bands [9]. In pressures higher than p_C ferromagnetic ordering in the Ho sublattice persists below T_C , which is usually almost pressure independent for ferromagnets consisting of localized magnetic moments. [9]. Paramagnetism survives up to 3 GPa while T_f and T_C have a similar pressure development. It leads to an idea of a common underlying mechanism of both phenomena – formation of long-range ferrimagnetic ordering and formation of short range paramagnetic configurations, which may be the Ho-Co exchange interaction.

Data from the μ SR experiment show also short-range correlations surviving above the flipping temperature T_f corresponding to the formation of Co ferromagnetic clusters, as it was reported in reference [12] for ErCo_2 . Figure 3 shows that λ_{slow} corresponds to paramagnetic fluctuations of Ho magnetic moments as it can be seen from the agreement of the values taken from HoAl_2 . The temperature T^* , at which the two exponentials (equation (2)) change to one exponential (equation (1)), corresponds to formation of Co magnetic clusters. This result confirms that Co magnetic clusters form at higher temperature than T_f . At flipping temperature T_f clusters begin interact with Ho magnetic moment. The loss of short-range-order correlations between Co magnetic moments is in contrast to proposed solution in reference [5], where there is proposed second paramagnetic regime in HoCo_2 above 150 K.

Figure 2 shows that T_f and T^* develop with pressure in the same manner. The Co magnetic clusters decay due to decreasing of correlation length between Co-Co. The external pressure influences the Co-Co exchange interaction and consequently the pressure dependence of T_f . Taking into account the pressure development of T_C leads to an idea of large dependence of T_C also on Co-Co exchange interactions through the following scenario. Assuming that the Ho-Co exchange is taking place rather between the localized Ho moment and the resulting magnetization of Co cluster - which is changing upon temperature development - the exchange between Ho-Co(clusters) is strongly dependent also on the internal Co-Co exchange within the cluster. This may explain the same pressure dependence of T_C , T_f and T^* .

Acknowledgements

This work was supported by the Czech Science Foundation under the project # P204/12/0692. It was also supported by the Grant SVV-2013-267303. Experiments were performed in MLTL (see: <http://mltl.eu/>) which is supported within the program of Czech Research Infrastructures (project LM2011025). The authors acknowledge the Swiss muon source ($\text{S}\mu\text{S}$) at Paul Scherrer Institute (PSI) for the granted beamtime.

References

- [1] Goto T, Fukamichi K, Sakakibara T and Komatsu H 1989 *Solid State Commun.* **72** 945
- [2] Cuong T D et al. 1998 *J. Magn. Magn. Mater.* **182** 143
- [3] Herrero-Albillos J et al. 2007 *J. Magn. Magn. Mater.* **316** 442
- [4] Herrero-Albillos J et al. 2007 *Phys. Rev. B* **76** 094409
- [5] Bonilla C M et al. 2012 *J. Appl. Phys.* **111** 07E315
- [6] Bonilla C M et al. 2013 <http://arxiv.org/abs/1302.0775>
- [7] Gignoux D, Givord F and Lemaire R 1975 *Phys. Rev. B* **12**, 3878
- [8] Houser R, Bauer E and Gratz E 1998 *Phys. Rev. B* **57** 2904
- [9] Syshchenko O et al. 2001 *J. Alloy. Compd.* **317** 438
- [10] Míšek M et al 2012 *J. Appl. Phys.* **111** 07E132
- [11] Kamarád J, Machátová Z and Arnold Z 2004 *Rev. Sci. Instrum.* **75** 5022
- [12] Bonilla C M et al. 2011 *Phys. Rev. B* **84** 184425

- [13] Hartmann O et al. 1986 *J. Phys. F: Met. Phys.* **16** 1593
- [14] Gignoux D et al. 1979 *J. Magn. Magn. Mater.* **10** 288